CHAPTER IV

RESULTS AND DISCUSSION

4.1 Synthesis and Characterization of Quaternized Chitosan (QCh)

Quanternization of chitosan was synthesized by using N-(3-chloro-2-hydroxypropyl) trimethylammonium chloride (NTMC), which is quaternary ammonium molecule. The reaction used iodine as a catalyst in process under alkaline conditions at pH 8 with sodium hydroxide which was effective in generating the epoxide from NTMC (Sajomsang *et al.*, 2009). The primary amino group of chitosan reacted with epoxide of NTMC molecule in a nucleophilic substitution pathway **(fig 4.1)** to introduce the quaternary ammonium group on the chitosan backbone. The quaternization of chitosan would improve water solubility in wide pH range.

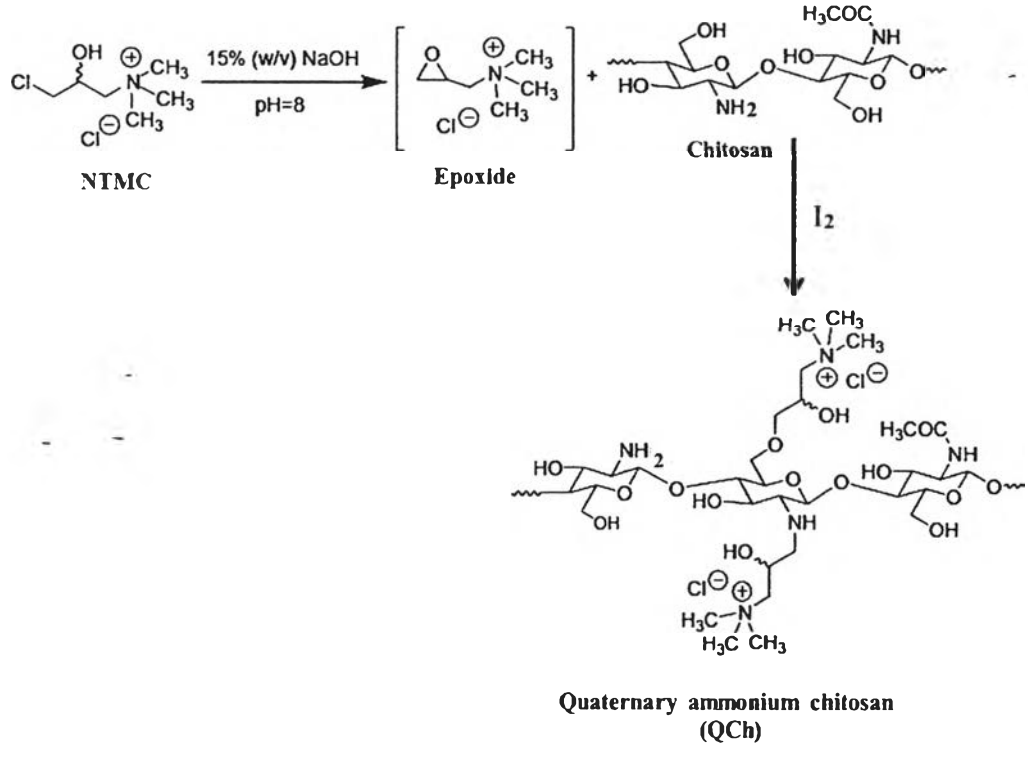

Figure 4.1 Synthesis of quaternary ammonium chitosan (QCh)

The chemical structures of chitosan (Ch) and quaternized chitosan (QCh) were characterized by FTIR and ^{1}H NMR spectroscopy. **Fig 4.2** shows the FTIR spectrum of Chitosan and QCh. The characteristics FTIR of Ch show the absorption band at wavenumber 1661 and 1600 cm^{-1} corresponded to the C=O of amide and N-H bending of primary amine, respectively. The absorption band at wavenumber of 3438 cm^{-1} corresponded to the OH and NH_2 group. Moreover, QCh exhibited absorption band at wavenumber 1560 cm^{-1} was the N-H deformation of amino groups due to primary amine became to secondary amine, while the absorption band at wavenumber 1145 and 1073 cm^{-1} corresponded to the symmetric C-O-C and C-O stretching. (Peng *et al.*, 2010, Sajomsang, 2010, Xu *et al.*, 2011)

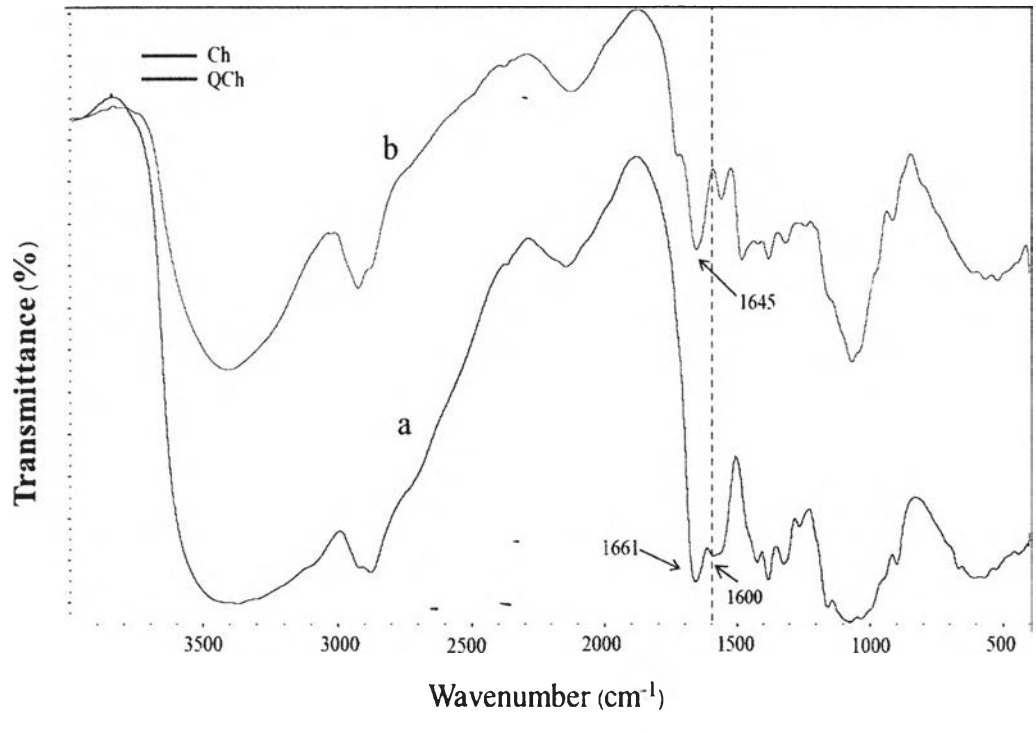

Figure 4.2 FTIR spectra of chitosan, Ch (a), and quaternized chitosan, QCh (b).

The ^{1}H NMR spectra of chitosan, NTMC and quaternized chitosan are present in **(Fig. 4.3a, 4.3b** and **4.3c)**, respectively. The ^{1}H NMR spectrum shows successful synthesized of quaternized chitosan comparing with chitosan and NTMC

spectrum. Chitosan **(fig. 4.3a)** exhibits characteristic signal at 1.9 ppm is attributed to the acetyl group of chitin. The characteristic peak of NTMC **(fig. 4.3b)** at 3.25 ppm is N,N,N-trimethyl proton .The characteristic peak of N,N,N-trimethyl proton (3.25 ppm) was presented in the spectrum of QCh, but absence from the spectrum of chitosan. (Sadeghi *et al.*, 2008, Sajomsang *et al.*, 2009, Peng *et al.*, 2010, Xu *et al.*, 2011).

The degree of quaternization (DQ) of QCh was calculated from the ^{1}H NMR spectrum data from **eq. 1.** The degree of quaternization of QCh was in a range of 72.0 ± 0.3 %.

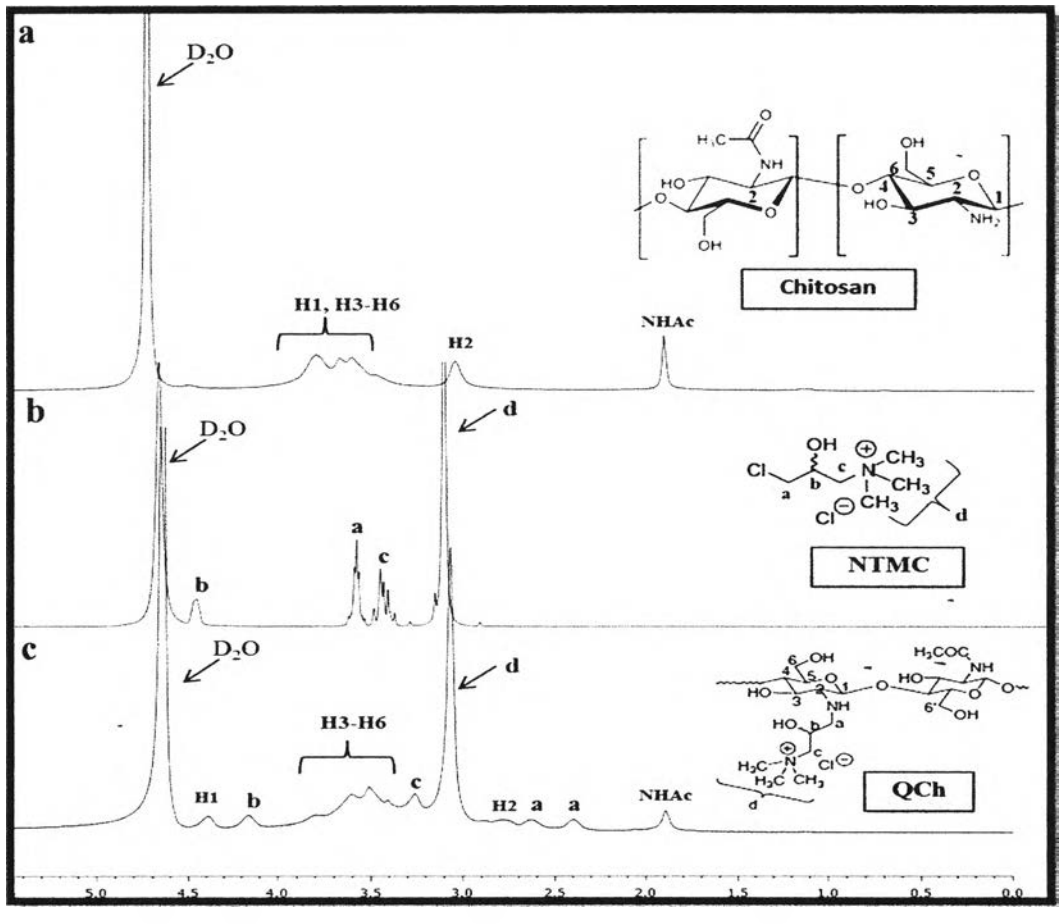

Figure 4.3 Shows ^{1}H NMR spectrum of chitosan (I), NMTC (II) and QCh (III).

4.2 Water Solubility of Quanternized Chitosan

The native chitosan cannot solute in water due to its strong intermolecular hydrogen bonds. The quaternization induced the positive charge, quaternized chitosan quaternary ammonium group; on the chitosan backbone with some steric and high hydrophilic group that can reduce the hydrogen bonding of chitosan. Therefore, chitosan become water-soluble molecule. The zeta potential was used to determine the positively charged surface of QCh and it related to portion of the chitosan that has been protonate and dissolved in water (Kong *et al.*, 2010). QCh had higher zeta potential than chitosan because NH_2-group or OH-group of chitosan converted to a quaternary ammonium group. Chitosan had zeta potential about 13 mV whereas QCh had zeta potential about 24-29 mV in distilled water. **Fig. 4.4** shows the pH dependence of the water solubility of chitosan and QCh from pH 3 to pH 13. At low pH (pH < 6), the transmittance of QCh is close to 100 % but the transmittance chitosan will slowly decrease to 70 %. This described that the chitosan and QCh molecules have good solubility in acidic solution. However, when the pH increases from 6.0 to 8.0, the transmittance of the chitosan solution rapidly declined from 70 % to 40 % and the solution becomes turbid.On the other hand, the transmittance of QCh solution slowly decreased and remained stable until pH 12. This result suggests that the QCh was good solubility in basic solution than chitosan.

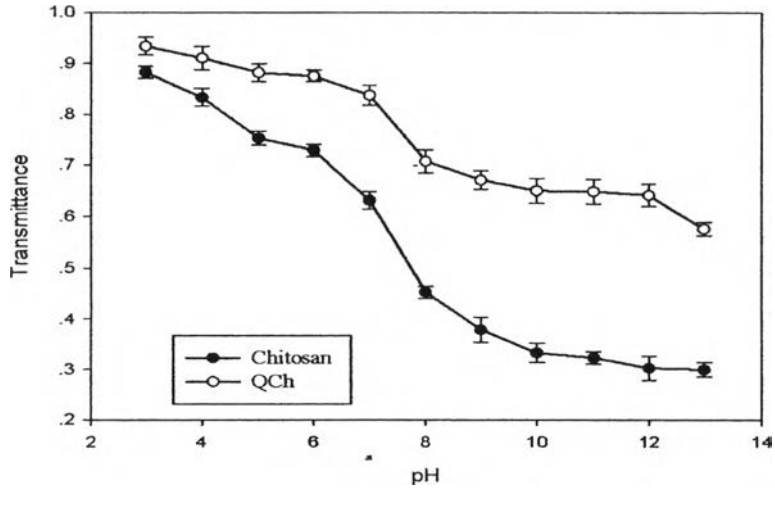

Figure 4.4 pH dependence of water solubility of chitosan and QCh.

4.3 Determination of MIC and MBC of Tetracycline

The antibacterial activity of tetracycline was determined by using standard protocol, broth dilution method, for evaluating the minimum inhibitory concentration (MIC) and minimum bactericidal concentration (MBC), which were the important values to confirm resistance of bacterial and also to evaluate the antibacterial activity of tetracycline. After determination of MIC and MBC, the concentration of tetracycline which can inhibit completely bacterial was selected as initial concentration loaded into QCh nanoparticles. **Table 4.1** shows MIC and MBC of tetracycline against *E.coli, E.faecium and S.aureus*, at pH 7.4.From resulting, the initial concentration of tetracycline was 2.5 mg/mL used to load into QCh nanoparticles due to its completely inhibition against all of three bacterial.

Table 4.1 MIC and MBC of tetracycline against *E.coli, S.sureus* and *Ent.faecium* by broth dilution method

Bacterial	Antimicrobials (mg/mL)	
	MBC	MIC
E.coli	0.049	0.024
S.aureus	0.012	0.012
Ent.faecium	1.56	0.781

4.4 Preparation of TC-loaded QCh Nanoparticles

4.4.1 Encapsulation Efficiency of TC-loaded QCh Nanoparticles

TC loaded QCh nanoparticles were prepared by the ionic crosslink between QCh (2.5 mg/mL) and TPP (0.5w/v) with difference ratios of QCh: TC from 1:1 to 1:5.The initial concentration of TC was 2.5 to 12.5 mg/mL. **Table 4.2** shows the effect of QCh: TC on the EE and size of QCh nanoparticles. The amount of TC loaded into nanoparticles was determined by UV-vis spectrophotometry at 270 nm and the encapsulation efficiency (EE) were calculated using **Eq.2**. The EE of TC was in a range of 72 – 95 %. In addition, the EE increased with increasing initial amount

of TC. The EE tended to increase because the electrostatic interaction between the negatively charged tetracycline and the positively charged quaternized chitosan are used as the driving force for the formulation of nanoparticles. This result was an agreement with (Wang *et al.*, 2010) that presented loading of anti-neuroexcitation peptide into TMC nanoparticles.

Table 4.2 Encapsulation efficiency (EE %) of TC-loaded QCh nanoparticles determined by UV-vis spectrophotometry and mean particles size of QCh nanoparticles and TC-loaded QCh nanoparticles by DLS

QCh:TC ratio	EE (%)	Mean particles size	
		nm	PDI
1:0	0	228 ± 25.9	0.778
1:1	72.44 ± 6.84	450 ± 73.2	0.822
1:2	84.05 ± 1.61	498 ± 14.8	0.736
1:3	92.01 ± 1.46	562 ± 47.5	0.652
1:4	92.48 ± 0.96	657 ± 26.0	1.000
1:5	94.18 ± 3.94	798 ± 44.5	0.601

(Results were reported as mean ± SD , n=3)

4.4.2 Shape and Size of TC-loaded QCh Nanoparticles

The size of QCh and QCh/TC nanoparticles were determined by dynamic light scattering (DLS) technique. **Table 2** shows that QCh nanoparticles possessed an average diameter of 228 nm.TC loaded QCh nanoparticles exhibited mean particles size in the range of 450 – 800 nm. The results could explain that the mean particles size increased with increasing initial TC content, which is concurrent to the findings of (Hosseini *et al.*, 2013).The mean particles size might be the hydrodynamic diameter of aggregate of single particles or the swelling of TC-loaded QCh particles around the individual particles (Yoksan *et al.*, 2010).The morphology of particles was observed by SEM. The SEM images **(Fig. 4.5)** of QCh nanoparticles

and TC-loaded QCh nanoparticles presented spherical shape, good distribution and smooth surface.

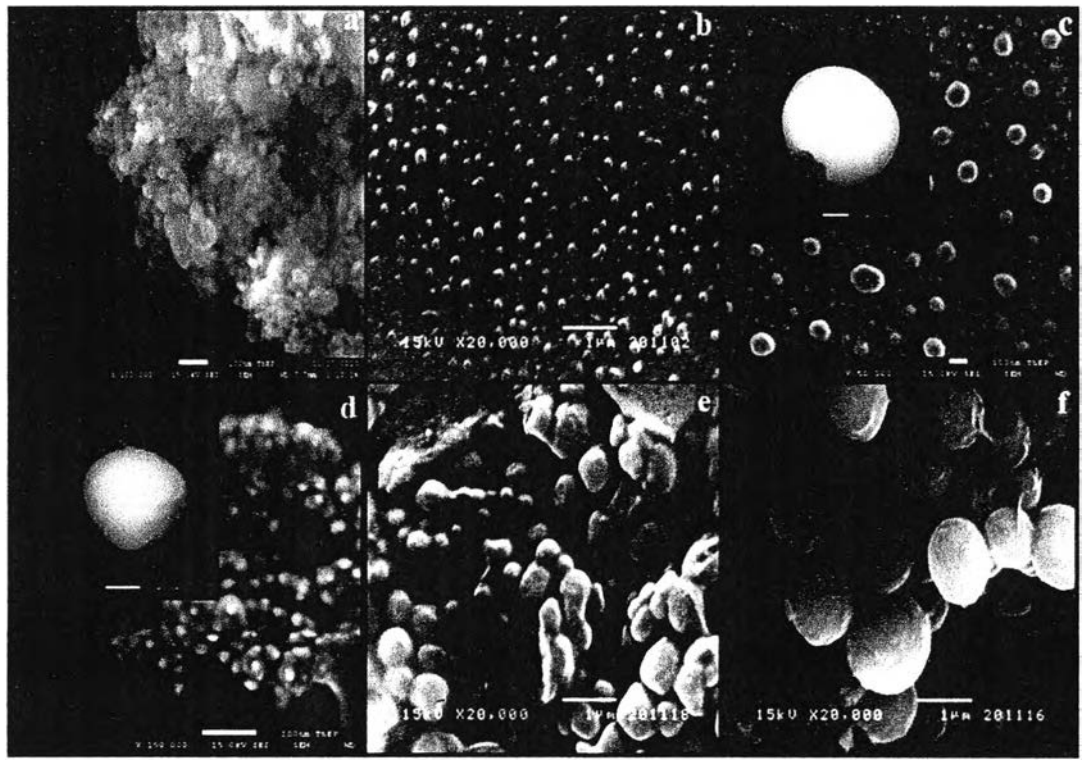

Figure 4.5 SEM images of QCh nanoparticles (a) and TC-loaded QCh nanoparticles ratio 1:1 (b), 1:2 (c), 1:3 (d), 1:4 (e) and 1:5 (f).

4.4.3 Confirmation of TC-loaded QCh Nanoparticles

Firstly, the technique that used to confirm the success of encapsulation was FTIR spectroscopy. The FTIR **(Fig.4.6)** of QCh show characteristics peak at 3438 cm^{-1} (OH and NH_2 group), at 2909 cm^{-1} (C-H stretching), 1652 cm^{-1} (C=O stretching), at 1560 cm^{-1} (deformation of $-NH_2$), at 1145 and 1073 cm^{-1} (C-O-C and C-O stretching) (Sajomsang, 2010, Xu *et al.*, 2011). In QCh nanoparticles, the peak at 2909 cm^{-1},1145 cm^{-1} and 1560 cm^{-1} were not found because the ionic cross link can enhance the entanglement of particles and peak of C=O shifted from 1656 cm^{-1} to 1633 cm^{-1} , implying the complex formation via electrostatic between $N^{+}(CH_3)$ of QCh and TPP within the nanoparticles. Peak of

TC-loaded QCh nanoparticles show peak at 2336 cm^{-1} was C-N stretching of tetracycline molecule, which can confirm tetracycline was loaded into QCh nanoparticles (Maya *et al.*, 2012).

Secondly, the success of encapsulation was confirmed by using UV-vis spectrophotometer in distilled water at 270 nm. The QCh and QCh/TC nanoparticles were dispersed in distilled water for 3 hours with stirred 300 rpm; the solution was collected and measured by UV-vis spectrophotometry. QCh nanoparticles showed no peak absorption bands at wavelength between 200 to 450 nm **(Fig.4.7a),** but TC-loaded QCh nanoparticles showed a maximum absorption band at wavelength of ~ 270 and ~ 355 nm **(Fig.4.7b-4.7d)** ,corresponding to TC reference **(Fig.4.7e).**Therefore , this can infer that TC was released from QCh nanoparticles, the encapsulation of TC in QCh nanoparticles were successfully. In addition, the absorption band at wavelength ~ 270 and ~ 355 nm increased with increasing amount of TC content.

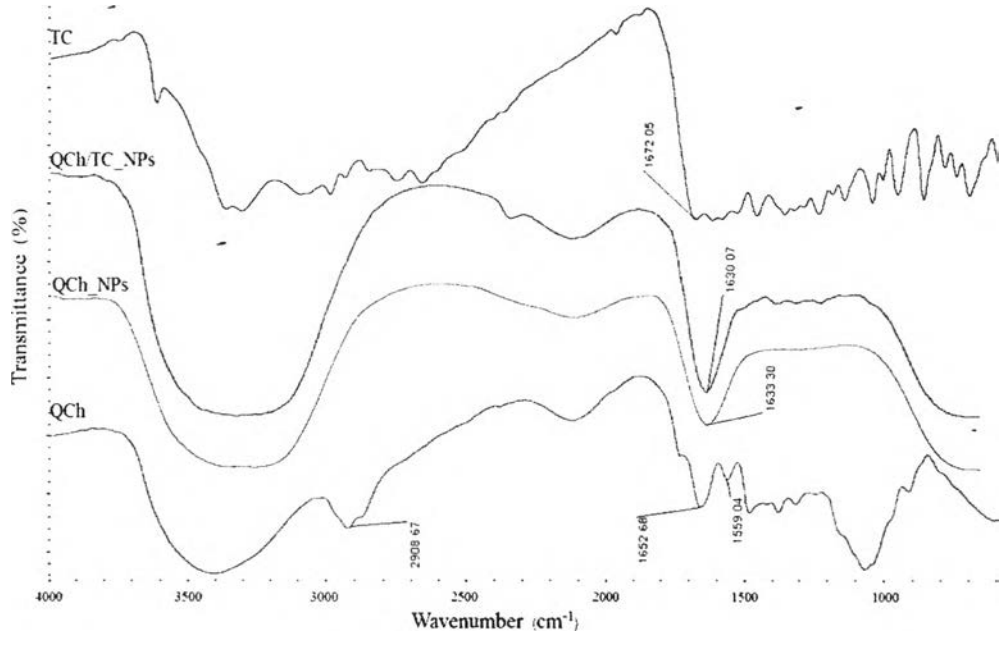

Figure 4.6 FTIR of QCh, QCh nanoparticles, TC-loaded QCh nanoparticles and tetracycline (TC) for confirming of success encapsulation.

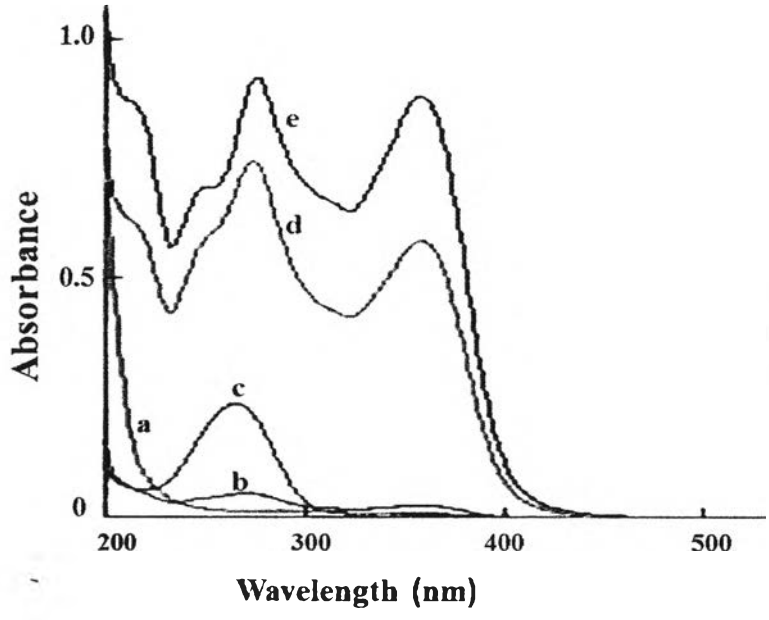

Figure 4.7 Uv-vis absorption band of solution obtained from dispersion of (a) QCh nanoparticles, QCh/TC nanoparticles of ratio (b) 1:1, (c) 1:2, (d) 1:3 and (e) tetracycline as reference.

Thirdly, the XRD was used to ensure completeness of TC-loaded QCh nanoparticles. The XRD pattern of QCh nanoparticles, TC, and TC–loaded QCh nanoparticles of ratio 1:3, 1:4, 1:5 are presented in **Fig.4.8**. TC showed many characteristic peaks at 2θ from 10° to 30°, which indicated the high degree of crystallinity .There are two characteristic peak of QCh nanoparticles at 2θ of 28° and 41° **(Fig.4.8a),** which similar presented in pattern of TC-load QCh nanoparticles of all ratio. As compare with QCh nanoparticles, the diffraction spectra of TC-load QCh nanoparticles presented characteristic peak at 2θ from 10° to 20° **(Fig.4.8b-4.8d),** which related with pattern of TC confirming the presence of TC within QCh nanoparticles (Yoksan *et al.*, 2010, Hosseini *et al.*, 2013).

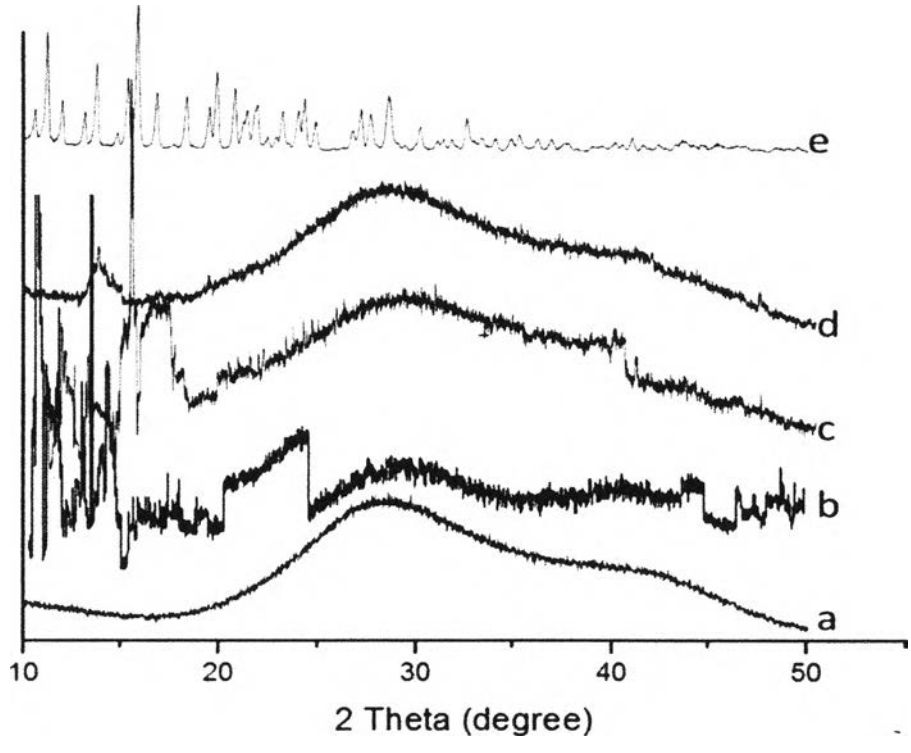

Figure 4.8 XRD patterns of (a) QCh nanoparticles, (b-d) QCh/TC nanoparticles of ratio (8b) 1:3, (8c) 1:4, (8d) 1:5 and (e) TC.

4.5 Preparation of Wound Dressing (PVA Film Blend with QCH/TC_NPs)

PVA films were prepared by solution casting method to obtain film that used as wound dressing. PVA blended with QCh nanoparticles which show transparent and colorless films **(Fig. 4.9a)**, but become to yellow films **(Fig. 4.9b, 4.9c)** when tetracycline loaded QCh nanoparticle.

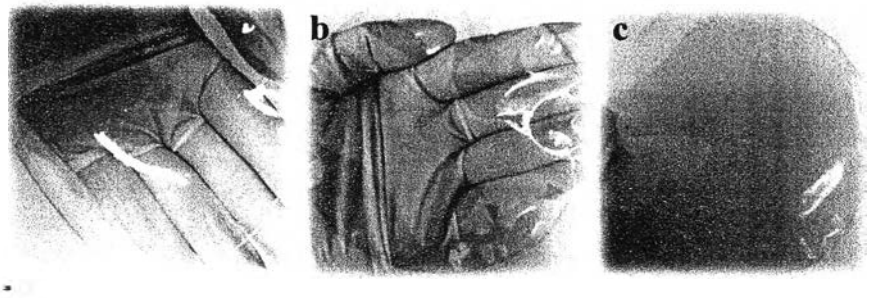

Figure 4.9 shows appearance of PVA film blend with QCh nanoparticles, (4.9a) and QCh/TC nanoparticles of ratio of 1:3, (4.9b) and 1:4, (4.9c).

4.5.1 *In vitro* Release Studies of Wound Dressing

The release profiles of tetracycline from QCh nanoparticles and PVA films, which prepare difference ratio QCh: TC. The drug release was determined in PBS buffer at pH 7.4 **(fig. 4.10a)** and Acetate buffer at pH 5.5 **(fig. 4.10b).**The amount of TC release from wound dressing was measured at 270 nm for PBS buffer and at 276 nm for Acetate buffer. The drug release from chitosan nanoparticles base on size, cross linking, morphology, and solubility of chitosan and the many mechanisms releasing can involve (a) release from the surface of particles, (b) diffusion through the swollen rubbery material and (c) release because polymer degradability (Agnihotri *et al.*, 2004). **Fig. 4.10** presented two stage of releasing, Firstly, the burst releases of TC were observed for the first 3 h from QCh nanoparticles of ratio (QCh: TC) 1:3, 1:4 ,1:5 about 12.8 %, 13.6 % ,13.9 % in PBS buffer and 13.7 %, 16.6 % , 13.8% in acetate buffer, respectively. This release of TC at this stage can involve the diffusion of TC at surface of particles (Keawchaoon *et al.*, 2011). Secondly, after 1 day has slower rate release of TC at this stage. The total concentrations of ratio 1:3, 1:4 and 1:5 were 24.7 %, 26.8 % and 20.2 % in PBS buffer and 24.1 %, 27.3 % and 19.3 % in acetate buffer, respectively. This can described toward the size of nanoparticles, in smaller particles, TC was a rapid released than bigger particles because small particles wound have greater surface-to-volume and mechanism at this stage was the diffusion of TC inside the nanoparticles due to the concentration gradient (Yoksan *et al.*, 2010). As a previous reported, (Hosseini *et al.*, 2013) the encapsulation of oregano essential oil in chitosan nanoparticles fast release within 4 hours and remain constant after 24 hours in different particles size. The pH of buffer did not have significantly effect to TC release due to good solubility of QCh in acid and natural media.

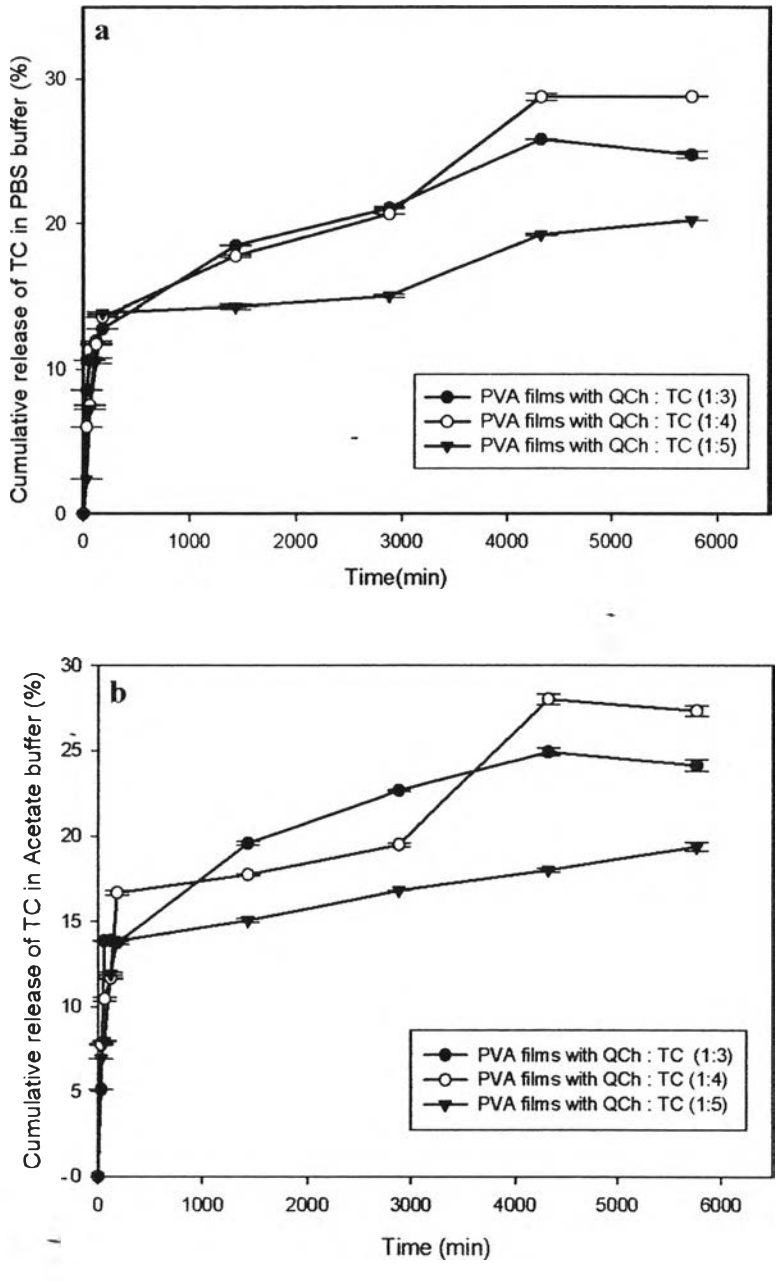

Figure 4.10 In vitro release of TC from QCh nanoparticle of ratio QCh: TC was 1:3, 1:4 and 1:5 in difference pH media (a) PBS buffer pH 7.4, (b) Acetate buffer pH 5.5. Result was reported as mean ± SD, n= 3.

4.6 Antibacterial Activity of Wound Dressing

4.6.1 Inhibition Zone

The method that used to determine was agar diffusion test, which the material cut to circle and placed on agar plate with incubating at 37 ^{0}C for 24 hours. **Table 4.3** presents the inhibition zone of wound dressing in difference ratio of QCh: TC against *E.coli, Ent.faecium* and *S.aureus*. The ratio of 1:1 and 1:2 that had TC-loaded QCh nanoparticle did not produce the inhibition zone. This can describe the ability of releasing of the drug from particles and polymer which amount of drug released less than MIC of each bacterial. On the other hand, wound dressing with ratios of 1:3, 1:4, and 1:5 have produced clearly inhibition zone against all of bacterial **(Fig.4.11)**. The inhibition zones which against *Ent.faecium* smaller than in case of *E.coli* and *S.aureus* due to drug resistance of bacterial. As expected, the wound dressing with QCh/TC nanoparticles have higher inhibitory effects than other ratio.

Table 4.3 Inhibition zone of wound dressing against *E.coli, Ent.faecium* and *S.aureus*

Bacterial	Inhibition zone (mm)				
	ratio of QCh : TC nanoparticles in wound dressing				
	1:1	1:2	1:3	1:4	1:5
E.coli	-	-	11.2 ± 0.6	11.5 ± 0.4	11.7 ± 0.2
S.aureus	-	-	13.5 ± 0.4	15.5 ± 0.2	16.0 ± 0.4
Ent.facium	-	-	5.5 ± 0.4	6.0 ± 0.5	6.5 ± 0.6

(-) Mean do not appear inhibition zone

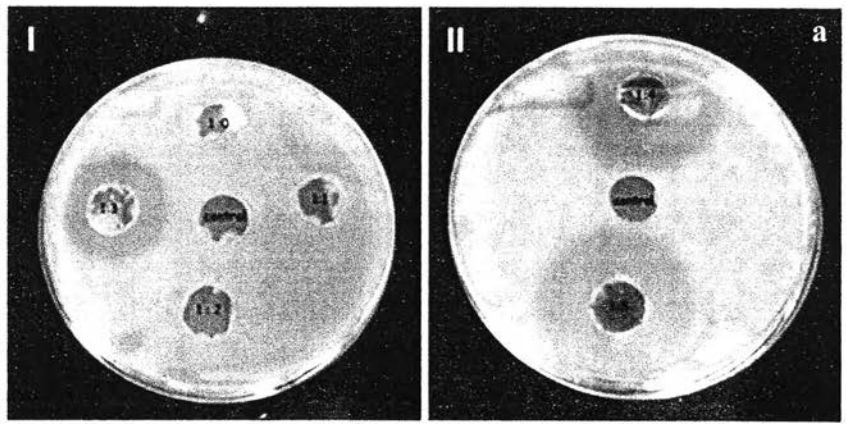

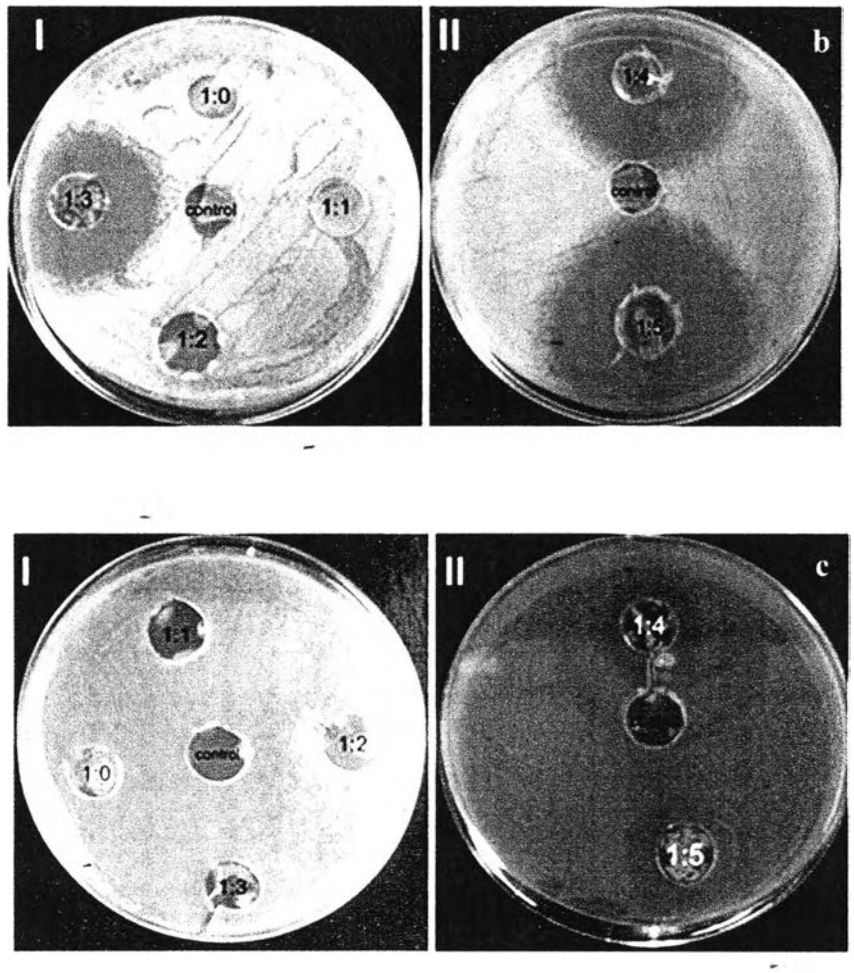

Figure 4.11 Inhibition zone of wound dressing of ratio QCh: TC of 1:3, 1:4 and 1:5 against *E.coli* (a), *S.aureus* (b) and *Ent.faecium* (c).

4.6.2 Percentage Reduction of Bacterial

The dynamic shaking method was used to determine the quantitative reduction of bacterial. The wound dressing materials of ratio 1:3, 1:4, and 1:5 were selected for percentage reduction testing due to their presenting of inhibition zones. The selected materials were shaken in the each bacterial medium (*E.coli*, *Ent.Faecium* and *S.aureus*) for 1, 3 and 24 hours at 110 rpm and at 37 ^{0}C. The antimicrobial activity is expressed in percentage reduction of the bacterial after contact with the PVA films compared to the number of bacterial surviving after contact with the control. The percentage reduction was calculated by using the following **Eq.5**. **Fig.4.12** presents percentage reduction of all bacterial dramatically

increased more than 90 % in 24 hours. This result can confirm that the wound dressing can release drug from QCh particles and polymer for killing bacterial.

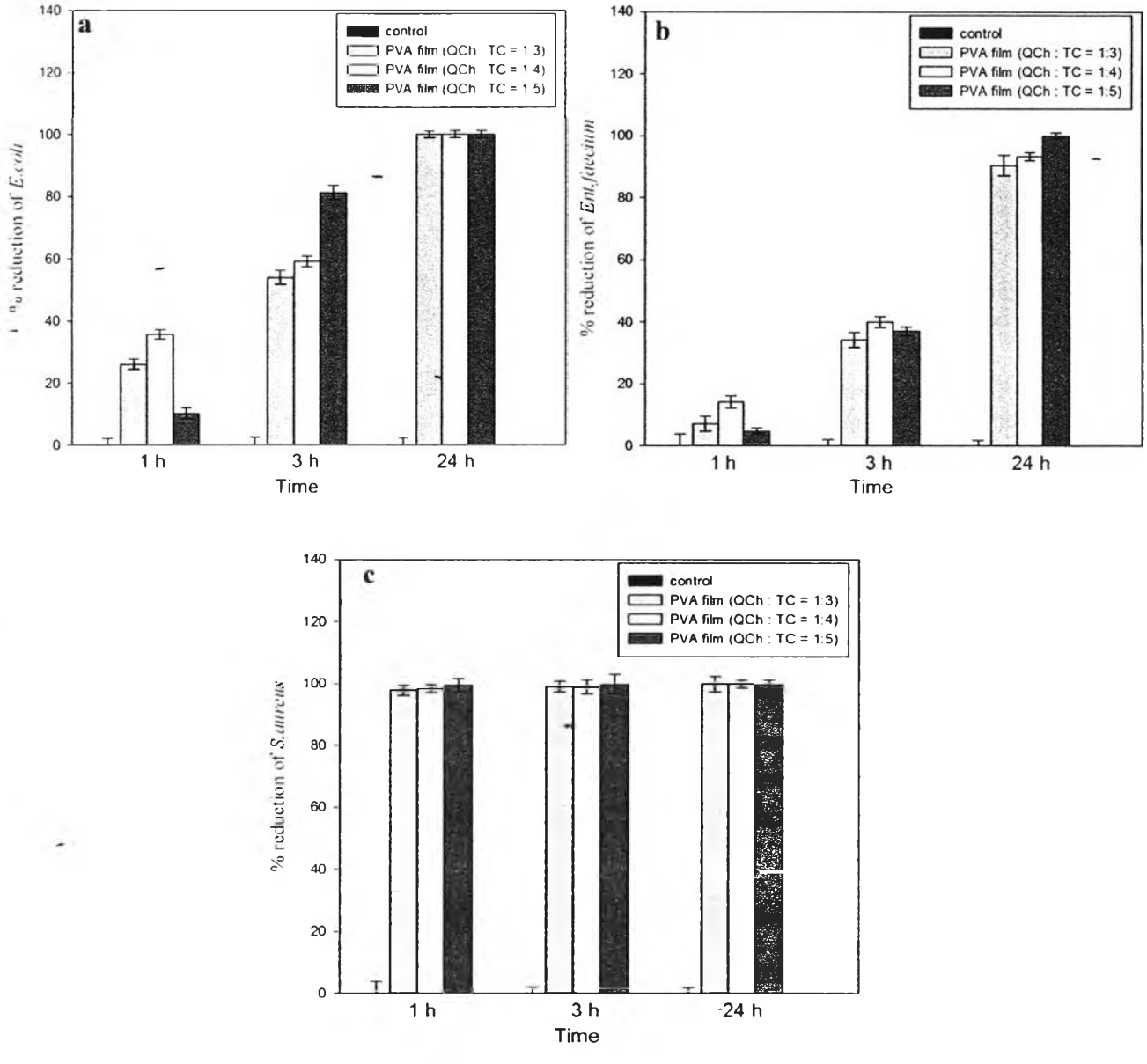

Figure 4.12 Ability of wound dressing for inhibition bacterial *E.coli* (a), *Ent.faecium* (b) and *S.aureus* (c).

4.7 *In vitro* Biocompatibility of Wound Dressing

The cytotoxicity is an importance factor to evaluate the viability of cells by detecting the toxic of material releasing. The cytotoxic effect of wound dressing was evaluated in L929 and FB cells for 1 and 3 days in order to obtain the release of drug

from wound dressing by using MTT assay. The MTT reagent composes of yellow tetrazolium salt that will turn to purple formazan crystal as it relate with the viability of cells. The viability of L929 **(Fig. 4.13a)** and FB cells **(Fig. 4.13b)** showed that only ratio of 1:3 (QCh: TC) more than 80 % cells were viable after 1 day and 3 day, signifying that these material are not cytotoxic and biocompatible.

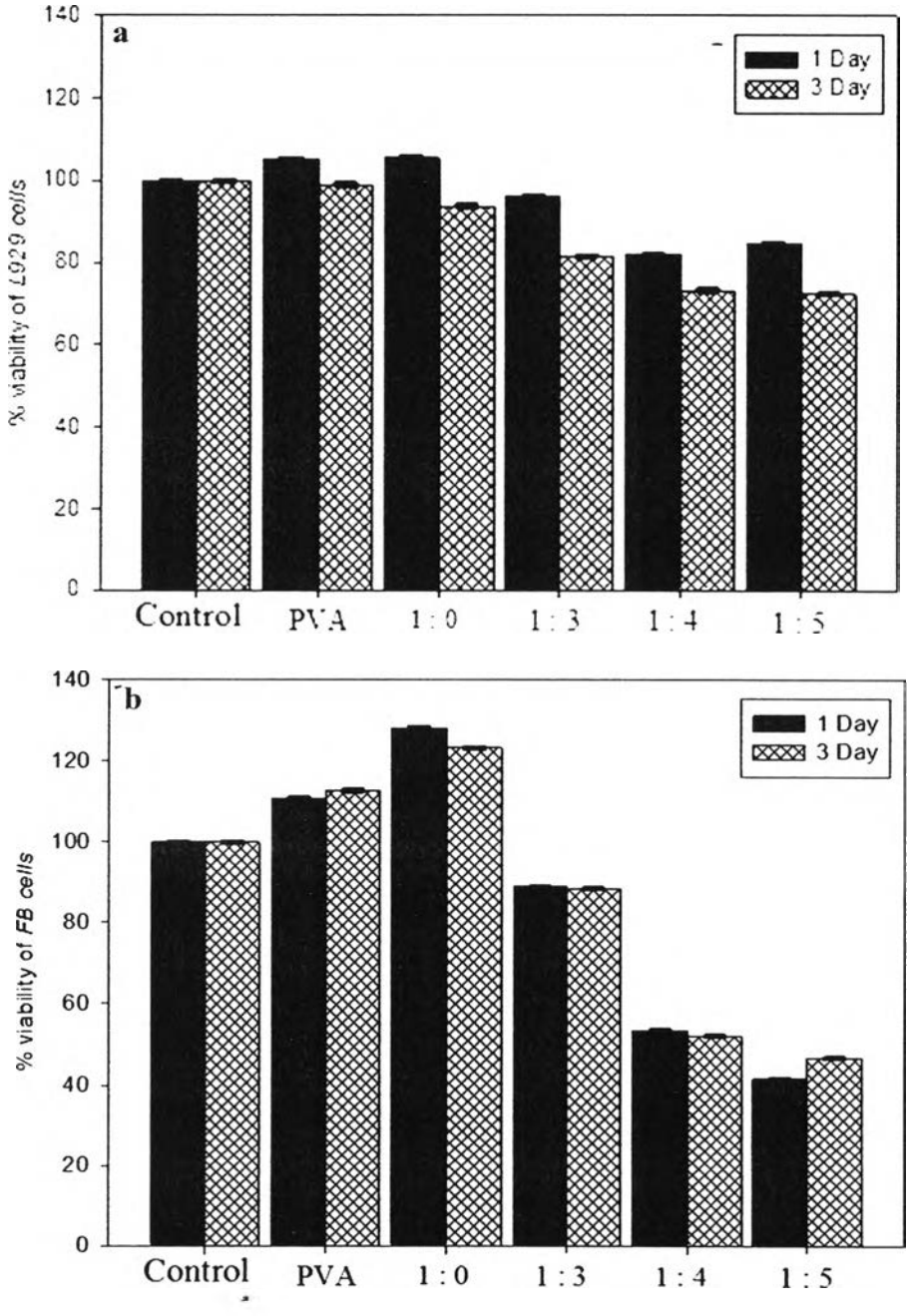

Figure 4.13 MTT assay were performed to detect the toxicity effect of wound dressing of ratio (QCh: TC) 1:0, 1:3, 1:4, 1:5 on *L929 cells* (a) and *FB cells* (b).